Influence of Zero-Field Splitting and State Mixing on Ferromagnetic Exchange in the Integrated-Stack Charge-Transfer Salt $[Cp^*_2Fe]^+[Co(HMPA\text{-}B)]^-$

David M. Eichhorn, Joshua Telser,† Charlotte L. Stern, and Brian M. Hoffman*

Department of Chemistry and Materials Research Center, Northwestern University, Evanston, Illinois 60208

*Received December 10, 1993**

We have prepared and studied the charge-transfer salts $[Cp^*_2M]^+[Co(HMPA\text{-}B)]^-$ (M = Fe (**1**), Co (**3**), Cp^* = pentamethylcyclopentadienyl, HMPA-B = bis(2-hydroxy-2-methylpropanamido)benzene). X-ray crystallographic analysis (orthorhombic *Pmmn*, a = 10.780(2) Å, b = 16.211(4) Å, c = 9.350(1) Å, V = 1634(1) Å^3, R = 0.034, R_w = 0.038) shows **1** to form integrated stacks where the $S=1/2$ $[Cp^*_2Fe]^+$ cation alternates with the planar $[Co(HMPA\text{-}B)]^-$ anion. Susceptibility measurements on **3**, which contains the diamagnetic $[Cp^*_2Co]^+$ cation, show that the Co^{III} of the anion exhibits a zero-field-split (D = 45 cm^{-1}) S = 1 electronic configuration. The situation in the two-spin crystal, **1**, is the inverse of that seen in the bulk ferromagnet $[Cp^*_2Mn]^+[TCNQ]^-$, where the cation has S = 1 and the anion has $S = 1/2$, but susceptibility measurements show that **1** does not order magnetically. Analysis of the interplay between exchange and a zero-field splitting (ZFS) on the anion indicates that **1** displays a substantial ferromagnetic coupling between cation and anion ($J \approx -7$ cm^{-1} where $H = JS_1 \cdot S_2$). However, this exchange is manifest as an increase in the apparent g-values of the cation that arises from quantum-mechanical state mixing in the presence of the large ZFS.

Introduction

The discovery that the integrated-stack $[D^+A^-]$ charge transfer (CT)[1] salt $[Cp^*_2Fe]^+[TCNE]^-$ is a molecular ferromagnet[2] initiated extensive efforts to understand the mechanism of ferromagnetic exchange coupling within decamethylmetallocenium salts.[3] As part of that effort, we demonstrated that replacement of the $S = 1/2$ $[Cp^*_2Fe]^+$ with the S = 1 manganese[4a] or $S = 3/2$ chromium[4b,c] analogs results in ferromagnets with higher values for the saturation magnetization, and others have expanded the list.[5] It was recognized that increasing the spin on either the anionic or cationic component would lead to higher critical temperatures (T_c), with $T_c \propto [S(S+1)]^{1/2}$ in the mean-field approximation providing that all else remains constant. However, T_c does not increase monotonically with spin in the series $[Cp^*_2M][TCNE]$, M = Fe ($S = 1/2$, T_c = 4.8 K),[2] Mn (S = 1, T_c = 8.8 K),[5a] and Cr ($S = 3/2$, T_c = 2.1 K).[4c] One possible explanation is that the crystal properties are influenced by a zero-field splitting (ZFS) of the high-spin ($S > 1/2$) ions, as described in the simplest version by the Hamiltonian

$$\hat{H} = D[\hat{S}_z^2 - 1/3(S(S+1))] \quad (1)$$

The influence of the ZFS on ferromagnetic ordering in a one-spin system has been addressed explicitly in the context of the quasi two-dimensional ferromagnet $Ni(SCN)_2(C_2H_5OH)_2$, which is based on the S = 1 Ni^{II} ion.[6] However, molecular magnets, in particular those based on the decamethylmetallocenium cation, commonly incorporate two paramagnetic components. When these have different values of the spin the effects of exchange couplings can be modified by quantum-mechanical state mixing. As part of an effort to explore the effects of zero-field splitting on the magnetic behavior of such binary spin materials we have extended our use of anionic metal complexes[7] by preparing and studying the charge-transfer salts $[Cp^*_2M]^+[Co(HMPA\text{-}B)]^-$ (M = Fe (**1**), Co (**3**)). X-ray crystallographic analysis shows

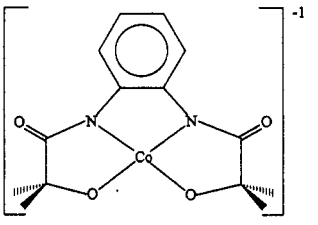

$[Co(HMPA\text{-}B)]^-$

that **1** forms integrated stacks where the $S = 1/2$ $[Cp^*_2Fe]^+$ cation alternates with the planar $[Co(HMPA\text{-}B)]^-$ anion. Susceptibility measurements on **3**, which contains the diamagnetic $[Cp^*_2Co]^+$ cation, confirm[8] that the Co^{III} anion exhibits an S = 1 electronic configuration. The situation in the two-spin crystal, **1**, is the inverse of that seen in the bulk ferromagnet $[Cp^*_2Mn]^+[TCNQ]^-$, where the cation has S = 1 and the anion has $S = 1/2$, but

† Permanent address: Department of Chemistry, Roosevelt University, Chicago, IL 60605.

* Abstract published in *Advance ACS Abstracts*, July 1, 1994.

(1) Abbreviations used: CT = charge transfer; Cp^* = pentamethylcyclopentadienyl; TCNE = tetracyanoethylene; ZFS = zero-field splitting; T_c = critical temperature; HMPA-B = 1,2-bis(2-hydroxy-2-methylpropanamido)benzene; TCNQ = tetracyanoquinodimethane; tdt = 1,2-toluenedithiol; bdt = 1,2-benzenedithiol; 3-Pr(bi) = 3-propylbiuret; TCA = trichloroacetate; TCAA = trichloroacetic acid.

(2) (a) Chittipeddi, S.; Cromack, K. R.; Miller, J. S.; Epstein, A. J. *Phys. Rev. Lett.* **1987**, *58*, 2695. (b) Miller, J. S.; Calabrese, J. C.; Rommelmann, H.; Chittipeddi, S. R.; Zhang, J. H.; Reiff, W. M.; Epstein, A. J. *J. Am. Chem. Soc.* **1987**, *109*, 769.

(3) (a) Kollmar, C.; Kahn, O. *Acc. Chem. Res.* **1993**, *26*, 259. (b) Gatteschi, D., Kahn, O., Miller, J. S., Palacio, F., Eds. *Molecular Materials*; NATO ASI Series; Kluwer Academic Publishers: Dordrecht, The Netherlands, 1991. (c) Kahn, O. *Struct. Bonding (Berlin)* **1987**, *68*, 89. (d) Miller, J. S.; Epstein, A. S.; Reiff, W. M. *Science* **1988**, *240*, 40.

(4) (a) Broderick, W. E.; Hoffman, B. M. *Science* **1990**, *249*, 401. (b) Broderick, W. E.; Hoffman, B. M. *J. Am. Chem. Soc.* **1991**, *113*, 6334. (c) Eichhorn, D. M.; Skee, D. C.; Broderick, W. E.; Hoffman, B. M. *Inorg. Chem.* **1993**, *32*, 491.

(5) (a) Yee, G. T.; Manriquez, J. M.; Dixon, D. A.; McLean, R. S.; Groski, D. M.; Flippen, R. B.; Narayan, K. S.; Epstein, A. J.; Miller, J. S. *Adv. Mater.* **1991**, *3*, 309. (b) Miller, J. S.; McLean, R. S.; Vazquez, C.; Calabrese, J. C.; Zuo, F.; Epstein, A. J. *J. Mater. Chem.* **1993**, *3*, 215.

(6) (a) DeFotis, G. C.; Harlan, E. W.; Remy, E. O.; Dell, K. D. *J. Appl. Phys.* **1991**, *69*, 6004. (b) Johnson, J. W.; Wang, Y.-L. *Phys Rev. B* **1981**, *24*, 5204. (c) Moriya, T. *Phys. Rev.* **1960**, *117*, 635.

(7) (a) Broderick, W. E.; Thompson, J. A.; Godfrey, M. R.; Sabat, M.; Day, E. P.; Hoffman, B. M. *J. Am. Chem. Soc.* **1989**, *111*, 7656. (b) Broderick, W. E.; Thompson, J. A.; Hoffman, B. M. *Inorg. Chem.* **1991**, *30*, 2958.

(8) Collins, T. J.; Richmond, T. G.; Santarsiero, B. D.; Treco, B. G. R. T. *J. Am. Chem. Soc.* **1986**, *108*, 2088.

0020-1669/94/1333-3533$04.50/0

Table 1. Crystallographic Data for $[Cp^*_2Fe]^+[Co(HMPA\text{-}B)]^-$

chem formula: $C_{34}H_{46}N_2O_4FeCo$	space group = *Pmmn* (No. 59)
fw = 661.53	T = −120 °C
a = 10.780 (2) Å	λ = 0.710 69 Å (Mo Kα)
b = 16.211 (4) Å	
c = 9.350 (1) Å	ρ_{calc} = 1.344 g cm^{-3}
V = 1634 (1) Å^3	μ = 9.87 cm^{-1}
Z = 2	R^a = 0.034
	$R_w{}^a$ = 0.038

^{a} $R = \Sigma||F_o| - |F_c||/\Sigma|F_o|$, $R_w = [\Sigma w(|F_o| - |F_c|)^2/\Sigma w|F_o|^2]^{1/2}$.

susceptibility measurements show that **1** does not order magnetically. Analysis of the interplay between exchange and a zero-field splitting (ZFS) on the anion indicates that **1** nonetheless displays a substantial ferromagnetic coupling between cation and anion. However, this exchange is manifest as an increase in the apparent g-values of the cation that arises from quantum-mechanical state mixing in the presence of the large ZFS.

Experimental Section

$[Cp^*_2Fe]^+[Co(HMPA\text{-}B)]^-$ (1). All reagents were used as received without further purification. Decamethylferrocene was prepared by literature methods,[9] oxidized by treatment with concentrated H_2SO_4, and precipitated as the hexafluorophosphate salt by addition of KPF_6. $PPh_4[Co(HMPA\text{-}B)]$ (**2**) was prepared by the method of Collins *et al.*[8] The charge-transfer salt, **1**, was synthesized by combining equimolar quantities of these two complexes in dichloromethane. Addition of hexanes resulted in the precipitation of a green powder, which was redissolved in methanol and filtered to remove PPh_4PF_6. The methanol was removed and the compound was redissolved in dimethylformamide. Slow diffusion of ether into this solution resulted in the deposition of dark green crystals of **1**. UV/Vis (CH_2Cl_2, λ_{max}, nm): 779,563,427,318,273. Anal. (Searle Laboratories, Skokie, IL) Found (calcd): C, 61.44 (61.73); H, 7.19 (7.01); N 4.22 (4.23).

$[Cp^*_2Co]^+[Co(HMPA\text{-}B)]^-$ (3). Decamethylcobaltocenium hexafluorophosphate was prepared by literature methods.[10] The charge-transfer salt, **3**, was prepared in a manner analogous to that for **1**.

Physical Methods. UV–visible spectra were recorded on a HP8452a spectrometer. Magnetic susceptibility data were collected on a Quantum Design MPMS magnetometer. Samples were contained in gelatin capsules and were suspended from the magnetometer probe within a length of heat-shrink tubing. Magnetic susceptibility data were corrected for core diamagnetism (calculated from Pascal's constants) and for diamagnetic contributions from the holder.

Fitting Programs. Magnetic susceptibility data were fit using a nonlinear least-squares fitting program, DSTEPIT,[11] linked to subroutines[12] that set up the spin Hamiltonian matrix for a given spin system, determine the energy levels, and calculate the powder susceptibility using the Van Vleck equation.[13]

X-ray Crystallography. A dark-green crystal of **1** with dimensions 0.34 × 0.17 × 0.16 mm, isolated as described above, was transferred directly from the mother liquor to Paratone-N oil, affixed to a glass fiber and placed in the cold stream of the CAD-4 diffractometer. The unit cell was determined from the setting angles of 25 reflections with 20° ≤ 2θ ≤ 22°. Further details are given in Table 1.

The data were corrected for Lorentz and polarization effects. No absorption correction was applied to the data. A correction for secondary extinction (0.55041 × 10^{-7}) was applied. The structure was solved by direct methods[14] and refined using the TEXSAN crystallographic software.[15] Non-hydrogen atoms were refined anisotropically. Hydrogen atoms were located on a difference Fourier map and their positions were refined with temperature factors set equal to 1.3 times the equivalent isotropic temperature factors for the carbon atoms to which they were attached.

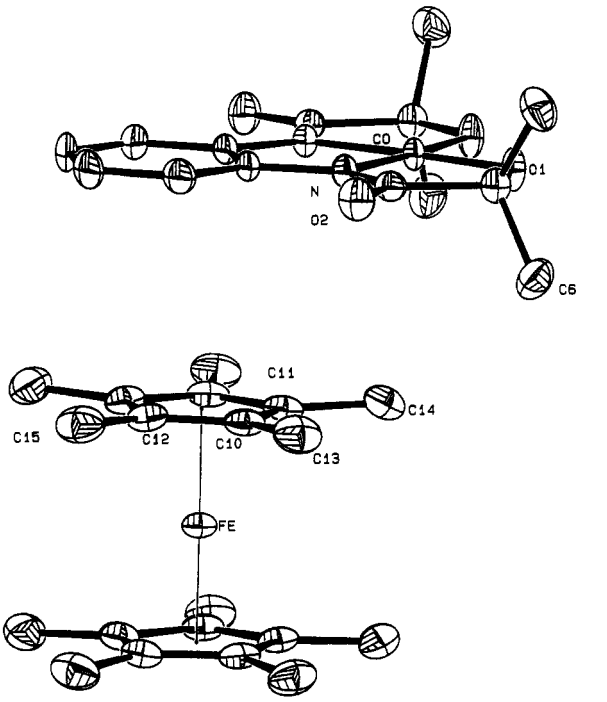

Figure 1. ORTEP drawing of **1** showing the 50% thermal ellipsoids. H atoms have been omitted for clarity.

Table 2. Positional Parameters and Equivalent Isotropic Temperature Factors for $[Cp^*_2Fe]^+[Co(HMPA\text{-}B)]^-$

atom	x	y	z	B_{eq} (Å^2)^a
Co	0.25	0.25	0.64900(7)	1.38(3)
Fe	0.25	0.75	0.02093(8)	1.56(3)
O(1)	0.25	0.3333	0.5232(2)	2.0(1)
O(2)	0.25	0.4671(2)	0.8299(3)	2.4(1)
N	0.25	0.3263(2)	0.7913(3)	1.5(1)
C(1)	0.25	0.2932(2)	0.9320(4)	1.6(1)
C(2)	0.25	0.3367(3)	1.0596(4)	2.2(2)
C(3)	0.25	0.2933(3)	1.1870(4)	2.6(2)
C(4)	0.25	0.4064(2)	0.7506(4)	1.7(1)
C(5)	0.25	0.4127(2)	0.5847	1.7(1)
C(6)	0.1343(3)	0.4581(2)	0.5381(3)	2.8(1)
C(10)	0.0913(2)	0.6788(2)	0.0601(3)	2.1(1)
C(11)	0.0923(3)	0.75	0.1515	2.1(2)
C(12)	0.0893(2)	0.7062(2)	−0.0849(3)	2.1(1)
C(13)	0.0847(3)	0.5907(2)	0.1085(4)	3.0(1)
C(14)	0.0876(4)	0.75	0.3121	3.1(2)
C(15)	0.0822(3)	0.6521(2)	−0.2138(4)	3.2(1)

^{a} $B_{eq} = (8\pi^2/3)\sum_{j=1}^{3} U_{ij} a_i^* a_j^* \vec{a}_i \vec{a}_j$.

Results and Discussion

Structure Description. Compound **1** crystallizes in the orthorhombic space group *Pmmn*. Figure 1 shows an ORTEP[16] drawing of one cation–anion pair displaying the relative orientation of the cation and anion within a stack. Positional parameters are given in Table 2 and selected bond angles and bond lengths are given in Table 3. Full structural data are given in the supplementary material. The individual cation and anion show no significant deviations from published structures.[8,17] The iron atom of the cation lies on a special position with *mm* site symmetry, one mirror plane relating the two Cp* rings and the other mirror plane bisecting each of the rings. This results in an eclipsed conformation of the Cp* rings, in contrast to the staggered configuration of the Cp* rings in $[Cp^*_2Fe]^+[TCNE]^-$ [2b] and the

(9) King, R. B.; Bisnette, M. B. *J. Organomet. Chem.* **1967**, *8*, 287.
(10) Robbins, J. L.; Edelstein, N.; Spencer, B.; Smart, J. C. *J. Am. Chem. Soc.* **1982**, *104*, 1882.
(11) DSTEPIT: Program #66, Quantum Chemistry Program Exchange, Department of Chemistry, Indiana University, Bloomington, IN 47401.
(12) Telser, J. Ph.D. Thesis, University of Florida, 1984. The updated, specific program versions used here are available from the authors.
(13) Carlin, R. L *Magnetochemistry;* Springer-Verlag: Berlin, 1986.
(14) Sheldrick, G. SHELXS-86, 1986.
(15) TEXSAN-TEXRAY Structure Analysis Package, Molecular Structure Corp., 1985.
(16) Johnson, C. K. ORTEPII. Report ORNL-5138. Oak Ridge National Laboratory, Oak Ridge, TN, 1976.
(17) (a) Miller, J. S.; Zhang, J. H.; Reiff, W. M.; Dixon, D. A.; Preston, L. D.; Reis, A. H.; Gebert, E.; Extine, M.; Troup, J.; Epstein, A. J.; Ward, M. D. *J. Phys. Chem.* **1987**, *91*, 4344. (b) Pickardt, J.; Schumann, H.; Mohtachemi, R. *Acta Crystallogr.* **1990**, *C46*, 39.

Table 3. Selected Interatomic Distances and Angles for $[Cp^*_2Fe]^+[Co(HMPA\text{-}B)]^-$

Intramolecular Distances (Å)			
Fe–C(10)	2.097(3)	Co–N	1.816(3)
Fe–C(11)	2.093(3)	Co–O(1)	1.791(2)
Fe–C(12)	2.118(3)		
Intramolecular Angles (deg)			
N–Co–N	85.8(2)	N–Co–O(1)	174.0(1)
O(1)–Co–O(1)	97.9(1)	N–Co–O(1)	88.2(1)
Intermolecular Distances (Å)			
Fe···Co (*a*-direction, intrastack)	6.211(1)	Co···C(14)	3.658(5)
Fe···Co (*b*-direction, interstack)	8.820(1)	C(6)···C(14)	4.367(5)
Fe···Co (*c*-direction, interstack)	8.264(1)	Cp* plane···benzene plane	3.65

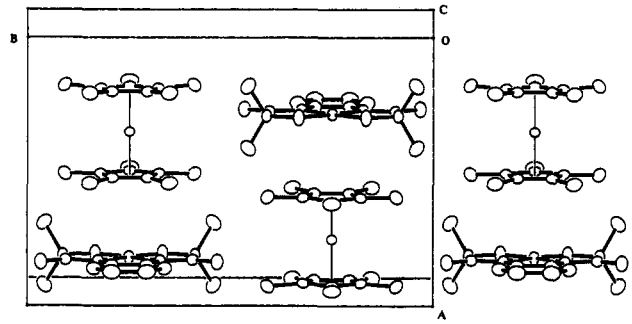

Figure 2. Crystal packing diagram for **1**.

1-D phase of $[Cp^*_2Fe]^+[TCNQ]^-$,[17a] but consistent with the eclipsed configuration of the metallocenium ions in $[Cp^*_2Fe][Br_3]$,[17b] $[Cp^*_2Mn]^+[TCNQ]^-$,[4a] $[Cp^*_2Cr]^+[TCNE]^-$,[5b] and the dimer phase of $[Cp^*_2Fe]^+[TCNQ]^-$.[17a] Similarly, the Co atom of the anion is situated on a special position with *mm* site symmetry, with one mirror plane containing the Co atom and the entire ligand (excluding the methyl groups C(6)) and the other mirror plane bisecting the ligand. This symmetry requires the ligand to be rigorously planar and the Co to lie in the plane of the ligand.

Figure 2 shows an ORTEP representation of the crystal packing of **1**, with selected intermolecular distances given in Table 3. The cations and anions form integrated stacks with donor and acceptor molecules alternating in the crystallographic *a*-direction. Within a stack, the Fe atom of the cation does not lie directly above the cobalt atom of an adjacent anion. Instead, the $[Cp^*_2Fe]^+$ cation is centered approximately above the benzene ring of the HMPA-B ligand, with one of the Cp* methyl groups (C14) almost directly above the Co atom. Thus, the Fe atom of the cation is offset from the line connecting the Co atoms of the two neighboring anions in the same stack. In the *c*-direction of the crystal lattice, the stacks are in phase with each other, a $[Cp^*_2Fe]^+$ cation in one stack situated adjacent to a $[Cp^*_2Fe]^+$ cation in each of the neighboring stacks, while in the *b*-direction the stacks are out-of-phase with each other, a cation in one stack next to an anion in each of the neighboring stacks.

The analogous compound, **3**, incorporates the diamagnetic $[Cp^*_2Co]^+$ cation and has been shown by single-crystal X-ray analysis to be isostructural to **1**.[18]

Magnetic Susceptibility. Magnetic susceptibility data for both **2** and **3** give a room-temperature magnetic moment of 3.4 μ_B, confirming the value reported by Collins and coworkers.[8] As shown in Figure 3, data for **2** and **3** taken over the temperature range 1.9–300 K can be fit in both cases to an $S = 1$ system described by the zero-field-splitting Hamiltonian of eq 1 with a large axial zero-field-splitting parameter, $D \approx 45 \pm 5$ cm^{-1}, where the Zeeman interaction has $g_\perp = 2.2(1)$, $g_\parallel = 2.5(3)$.[19] The value for D is of the same order as those reported for other square-planar Co^{III} species, such as $[NBu_4][Co(tdt)_2]$ (39 cm^{-1}),[20] $[NBu_4][Co(bdt)_2]$ (37 cm^{-1}),[20] and $KCo(3\text{-}Pr(bi))_2$ (41 cm^{-1}).[21]

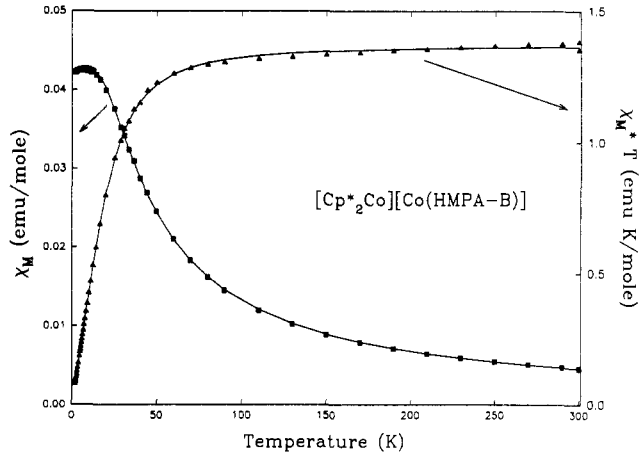

Figure 3. Magnetic susceptibility data for **3** plotted as χ_m (■) and $\chi_m T$ (▲). Solid lines represent a fit where $D = 45$ cm^{-1} (eq 1) and the Zeeman interaction has $g_\perp = 2.2$ and $g_\parallel = 2.5$.

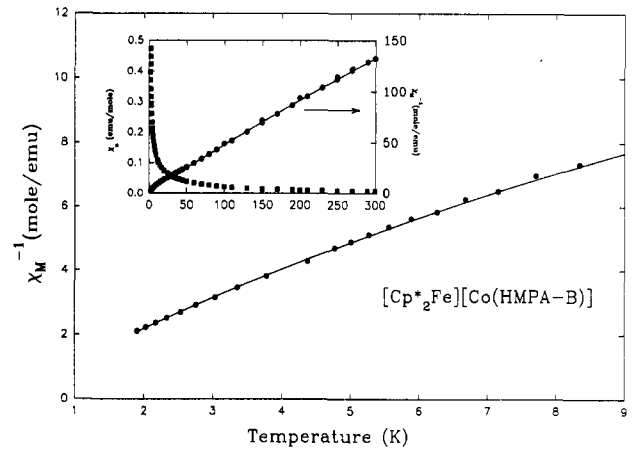

Figure 4. Magnetic susceptibility data for **1** plotted as χ_m^{-1} for $T < 10$ K. Inset: Susceptibility data for **1** plotted as χ_m (■) and χ_m^{-1} (●) for 1.9 K $< T <$ 300 K. Solid lines represent a fit to a ferromagnetically coupled model described by the ZFS Hamiltonian (eq 1) with $D = 45$ cm^{-1}, an isotropic exchange interaction ($H = JS_1 \cdot S_2$) with $J = 7$ cm^{-1} and Zeeman interaction parameters $g_\perp^{Fe} = 1.41$, $g_\parallel^{Fe} = 4.40$, $g_\perp^{Co} = 2.2$, and $g_\parallel^{Co} = 2.4$.

Figure 4 shows magnetic susceptibility data for **1**, plotted as χ_M^{-1} vs T for $T < 10$ K. In the inset, data taken over the full temperature range 1.9–300 K are plotted as χ_M vs T and χ_M^{-1} vs T. Clearly, bulk ferromagnetism is not achieved in this system, as there is no abrupt increase in the susceptibility at low temperatures, and it must be concluded that the coupling between the $[Co(HMPA\text{-}B)]^-$ acceptor and the $[Cp^*_2Fe]^+$ donor is not large enough to overcome the large positive D.

The first step in analyzing the magnetic susceptibility data for **1** was to use a model of non-interacting spins, $S^{Co} = 1$ and S^{Fe}

(18) Unit cell parameters: orthorhombic, $a = 16.28(2)$ Å, $b = 9.38(1)$ Å, $c = 10.60(1)$ Å.
(19) The errors given for the fit parameters represent an estimate of the variation obtained for different initial values.
(20) van der Put, P. J.; Schilperoord, A. A. *Inorg. Chem.* **1974**, *13*, 2476.
(21) Birker, P. J. M. W. L.; Bour, J. J.; Steggerda, J. J. *Inorg. Chem.* **1973**, *12*, 1254.

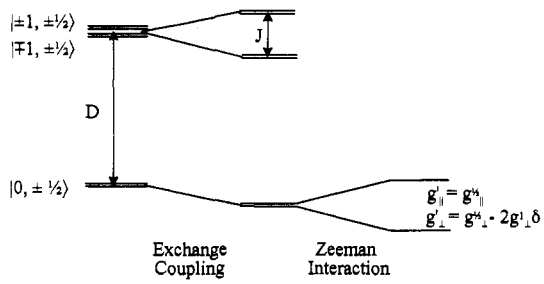

Figure 5. Effects of zero-field splitting (D) and exchange coupling (J) on the energy levels for a binary pair of $S = 1$ and $S = {}^1/_2$ spins.

$= {}^1/_2$. As a starting point, the susceptibility of **1** was calculated assuming the $S = 1$ Co^{III} anion had the parameters determined for **2** and **3** and the $S = {}^1/_2$ $[Cp^*_2Fe]^+$ cation had the g values reported for $[Cp^*_2Fe]PF_6$ ($g_\perp = 1.35$, $g_\parallel = 4.40$).[22] However, this gave a poor fit to the observed data. Next, the magnetic parameters of the individual spin systems were allowed to vary, with the above quoted values for anion and cation chosen as initial guesses. The best-fit values for this model are $D = 45 \pm 5$ cm^{-1}, $g_\perp{}^{Fe} = 1.95 \pm 0.05$, $g_\parallel{}^{Fe} = 4.40 \pm 0.02$, $g_\perp{}^{Co} = 2.1 \pm 0.1$, and $g_\parallel{}^{Co} = 2.5 \pm 0.2$, and they lead to values of $\chi(T)$ that accurately reproduce the experimental data (not shown). The parameters defining the Co^{III} system do not differ significantly from those of the anion in **3**. However the best-fit value for $g_\perp{}^{Fe}$ shows an unacceptably large deviation from that of the isolated cation (1.35)[22] as well as other symmetrically substituted ferrocenium species, $[Cp_2Fe]PF_6$ ($g_\perp = 1.26$)[22] and $[Cp^*_2Fe][TCA]\cdot 2TCAA$ ($g_\perp = 1.26$).[22] Clearly, the model of non-interacting $S = 1$ and $S = {}^1/_2$ spins can *describe* the susceptibility data, but does not *explain* it.

The explanation lies with the recognition that quantum mechanical state mixing caused by exchange coupling (defined here by the isotropic exchange Hamiltonian, $H = JS_1\cdot S_2$) between an $S = 1$ ion with large D and an $S = {}^1/_2$ ion manifests itself as an *apparent* change in the g-values of the $S = {}^1/_2$ ion when the data are modeled as a system of noninteracting spins. To understand this phenomenon, consider an isolated pair of $S = 1$ and $S = {}^1/_2$ spins. When $\delta \equiv J/D < 1$ such a system exhibits six energy levels (Figure 5). The ground state is a simple Kramers doublet derived from the $m_s = 0$ state of the $S = 1$ species and the $m_s = \pm{}^1/_2$ states of the $S = {}^1/_2$ species abbreviated as $|0\pm\rangle \equiv |0,\pm{}^1/_2\rangle \equiv |1,0\rangle\,|{}^1/_2,\pm{}^1/_2\rangle \equiv |S_1, m_{S_1}\rangle\,|S_2, m_{S_2}\rangle$. Two excited state doublets derived from the $m_s = \pm 1$ states of the $S = 1$ species are separated by $\Delta \approx D$ from the ground doublet. At low temperature ($D/kT \gg 1$) only the ground doublet is populated; the $S = 1$ species is nonmagnetic and the observed susceptibility is due only to the $S = {}^1/_2$ species. However, an exchange coupling between the spins perturbs the ground doublet by mixing in the higher-lying states $|+1,-{}^1/_2\rangle$ and $|-1,+{}^1/_2\rangle$. This induces a net magnetic moment on the $S = 1$ site. The additional interaction of this moment with the external field shifts the g-value of the ground-state doublet of the pair, giving

$$g_\parallel{}' = g_\parallel{}^{1/2} \tag{2a}$$

$$g_\perp{}' = g_\perp{}^{1/2} - 2g_\perp{}^{1}\left(\frac{J}{D}\right) \tag{2b}$$

$$= g_\perp{}^{1/2} - 2g_\perp{}^{1}\delta$$

If this treatment is extended to an alternating linear chain of spins in which each spin has z (=2) neighbors of the opposite type, eq 2b becomes:

$$g_\perp{}' = g_\perp{}^{1/2} - 2zg_\perp{}^{1}\delta \tag{3}$$

In a fit modeled upon noninteracting spins, these shifted $g_\perp{}'$ values would be assigned to the $S = {}^1/_2$ species, namely to $g_\perp{}^{Fe}$ for **1**, thereby leading to apparent anomalies. In particular, ferromagnetic coupling (J, $\delta < 0$) leads to an *increase* in $g_\perp{}'$, precisely as seen in our independent-spin fits for **1**; antiferromagnetic coupling leads to an analogous decrease.

The situation becomes more complicated as T is increased and other states become populated. An heuristic picture of the full temperature dependence of the magnetic behavior of **1** is obtained by treating the chain as being comprised of discrete dimers. The magnetic susceptibility data for **1** was thus fit using a model that includes exchange coupling between the two spins. Using values determined for the parent ions as initial guesses, the data were accurately fit by this model (Figure 4) with best-fit parameters $J = -7.0$ cm^{-1}, $D = 45$ cm^{-1}, $g_\perp{}^{Fe} = 1.41$, $g_\parallel{}^{Fe} = 4.40$, $g_\perp{}^{Co} = 2.2$, and $g_\parallel{}^{Co} = 2.4$.[23] Now all the parameters, including $g_\perp{}^{Fe}$, are consistent with their parent-ion values, and thus the variable-temperature magnetic susceptibility data for **1** can be explained by ferromagnetic coupling between the two components without perturbation of their individual electronic structures. Moreover, the values of J and D obtained from the fit give $\delta \approx -0.16$, which yields (eq 2b) $\Delta g_\perp{}^{Fe} \approx 2g_\perp{}^{Co}\delta \approx 0.7$. This agrees quite well with the shift of ≈ 0.5 calculated above when the susceptibility of **1** is fit with a model of noninteracting spins. Clearly this spin-coupling model captures the essential features of the magnetic interactions in **1**.

Discussion. The planar anionic metal complex $[A^-] = [Co(HMPA\text{-}B)]^-$ forms alternating-chain CT salts with metallocenium cations. Although **1**, the salt with $D^+ = [Cp^*_2Fe]^+$, does not exhibit bulk magnetic ordering, our results show the presence of a significant intrastack ferromagnetic exchange interaction, $J \sim -7$ cm^{-1}. In the absence of such an interaction a large positive zero-field splitting ($D \sim 45$ cm^{-1}) would cause the Co^{III} ($S = 1$) anion to be nonmagnetic at low temperature. However, the ferromagnetic D^+–A^- exchange causes state mixing that induces a magnetic moment on the $[A^-]$ species. This is reflected in an increase in the g-value for the spin-coupled $[D^+A^-]$ system that *appears* as a shift in $g_\perp$ for the ($S = {}^1/_2$) $[Cp^*_2Fe]^+$ ion. Intriguingly, this solid-state system is electronically similar to compound I of the metalloenzyme catalase, in which an $S = 1$ oxoferryl is ferromagnetically coupled ($J < 0$) to an $S = {}^1/_2$ porphyrin cation radical.[24] The enzyme exhibits a ground-state doublet whose observed value of $g_\perp$ is shifted from $g_\perp \approx g_e$ to $g_\perp = 3.3$, corresponding to $\delta = J/D \approx -0.4$.

An inference to be drawn from these considerations is that a large ZFS does not *necessarily* preclude magnetic ordering in a binary spin system where the high-spin component has integer spin. The mean-field theory of ferromagnetism suggests that for a binary chain comprised of alternating high-spin ($S_1 > {}^1/_2$) and low-spin ($S_2 = {}^1/_2$) components, T_c should increase with S_1 in the absence of a ZFS: $T_c \propto J\langle S_1\rangle \propto J[S_1(S_1+1)]^{1/2}$. For a homospin system with $S_1 = S_2 = 1$, for a given J there is a critical value of $|\delta|$, below which magnetic ordering is precluded.[6] However, in a binary-spin system with $S_1 = 1$ and $S_2 = {}^1/_2$, state mixing by exchange between the two components induces a nonzero spin on the former such that $\langle S_1\rangle \approx |\delta|$. Thus, magnetic ordering should remain a possibility even for small δ, but with $T_c \propto J|\delta|$.

Future work will extend the attempt to understand the magnetic behavior of integrated chains with unequal component spins and in particular the interplay between zero-field splitting and exchange coupling.

Acknowledgment. This work has been supported by the Solid State Chemistry Program of the National Science Foundation

(22) Duggan, D. M.; Hendrickson, D. N. *Inorg. Chem.* **1975**, *14*, 955.

(23) Fit includes a temperature-independent-paramagnetism (TIP) of 8×10^{-4} emu/mol.

(24) Benecky, M. J.; Frew, J. E.; Scowen, N.; Jones, P.; Hoffman, B. M.; *Biochemistry* **1993**, *26*, 11929.

through Grant No. DMR-9144513 (B.M.H.) and benefited from support by the Northwestern University Materials Research Center, Grant No. DMR-9120521. We thank Dr. Peter Doan for helpful discussion.

Supplementary Material Available: Tables of positional parameters and temperature factors, and full listings of intramolecular bond distances and angles and intermolecular bond distances (8 pages). Ordering information is given on any current masthead page.